CHALMERS

Truck Frontal Underride Protection – Compatibility Factors Influencing Passenger Car Safety

Aleksandra Krusper

Department of Applied Mechanics, Chalmers University of Technology, Gothenburg, Sweden

Robert Thomson

Swedish National Road and Transport research Institute (VTI), Gothenburg Sweden

Aleksandra Krusper

P.O.Box 8077

SE-402 78 Gothenburg, Sweden

Tel.: +46(0)31 772 36 52

Fax: +46(0)31 764 71 88

E-mail: aleksandra.krusper@chalmers.se

Truck Frontal Underride Protection – Compatibility Factors Influencing Passenger Car Safety

Abstract

Frontal collisions between passenger cars and trucks are the most severe vehicle-vehicle collisions observed in accident statistics. Regulation 93 was developed to reduce the risk of fatal injury by preventing passenger cars from underriding heavy truck structures. The regulation does not fully address the higher energy of content in these collisions where passenger car structures cannot be expected to have sufficient energy absorbing capacity. The performance of a FUPD incorporated into a FE truck model was evaluated and compared to earlier studies by the authors. In particular, structural interaction of the car with the truck structures was investigated. The packing of the FUPD and truck structures was a critical factor for the FUPD performance. It was found that when the vertical offset between the FUPD truck frame rails is too small, the efficiency of the FUPD is decreased. Incorporating deformable truck frame elements is only beneficial if the offset is at least 220 mm.

Keywords: frontal crash, front underrun protective device; compatibility, heavy goods vehicles, FEM

Introduction

Frontal collisions between passenger cars and Heavy Goods Vehicles (HGV) are the most severe vehicle-vehicle collisions observed in accident statistics (Rechnitzer 1993; NHTSA 1998; Schäfer et al. 1999). The reason can be attributed to the great difference between the structure and mass (and thereby stiffness) of the two types of vehicles. Directive 2000/40/EC was developed to reduce the risk of fatal injury by preventing passenger cars from underriding truck structures and thereby reducing the severity of the frontal crashes. The directive demands that all trucks produced after

August 2003 are equipped with a Front Underrun Protective Device (FUPD) obeying requirements given by Economic Commission for Europe Regulation No. 93 (ECE-R93). Although this countermeasure can improve the interaction between the vehicles, the regulation does not fully address the higher energy content in these collisions where passenger car structure cannot be expected to have sufficient energy absorbing capacity. The Regulation has been criticized for specifying low stiffness requirements for the FUPD**.** The problem of insufficient bending stiffness of FUPD beam has also been reported in in-depth car to truck accidents analysis (Krusper and Thomson 2008). A statistical accident analysis has shown that closing speeds for fatal injuries are generally above 80 km/h (Schram et al. 2006). For reference, passenger car frontal protection in ECE Regulation 94 was based on closing speeds of 100 km/h (EEVC 1996). The accident analysis in VC-COMPAT showed that more collisions occur for horizontal overlaps where less than 50% of a truck and 75% of a vehicle fronts are involved (Gwehenberger 2003) and is in agreement with another accident investigation (EEVC WG 14 1996) where horizontal overlap of 75% and 75 km/h closing speed was found as a typical crash configuration. Closing speeds above 80 km/h were found as the limit speed after which fatalities begin to be noticeable in the data. Fatal accidents represent 50% of accidents with closing speeds around 130 km/h (Gwehenberger et al. 2003). The greatest proportion of impacts lies in the 12 o'clock (+/- 15 deg) category with impacts of larger angles being less common. It is important to note that closing speeds of 100 km/h are easily achieved in urban traffic. Already in 1993 energy absorbing FUPD has been proposed as a further step in improving passenger car's occupant protection (Rechnitzer 1993).

Although some car to truck tests with energy absorbing FUPD have been performed either sufficient data to evaluate e.a. FUPD were not given (Forsman 2002)

or the energy absorbing parts of FUPD were not triggered. However, all tests were run with 75% horizontal overlap and 100% vertical overlap. The only test where an e.a. FUPD showed desired performance was done within VC-COMPAT project with specially designed FUPD. A crash configuration for this test was planned in the way which did not allow contact between stiff parts of the passenger car (engine and gear box) and corresponding truck stiff structures resulting in 110 mm FUPD protrusion outside of truck's front and 400 mm of its gross rearward displacement. Horizontal and vertical overlaps were 72% and 100% respectively. Although one of the trucks considered in the in-depth accident analysis (Krusper and Thomson 2008) was equipped with e.a. FUPD, its performance could not be analyzed. MADYMO models (EEVC WG14) were used to simulate car-truck impact with e.a. FUPD with closing speeds of 56, 75 and 90 kmh^{-1}. Deformation distances for FUPD were 50, 160, 360 and 480 mm with 200kN crush triggering force and 400-600kN maximum force. Horizontal and vertical overlaps were 75% and 100% respectively for all simulations. Based on forces and deformations registered on dummies (no intrusions could be simulated) it was found that the optimal deformation length for the FUPD is around 360 mm. Another two sets of car – truck crash simulations based on FEM (Finite Element Method) were run within the VC-Compat project (Schram 2005 D14). The closing speeds of 56, 75 and 90 km^{-1} were combined with 50, 75 and 100% horizontal overlaps under full vertical overlap. In the first set of simulations four trucks were used for each combination: one model represented the trucks currently on the roads and three other models which some stiff parts were removed on the front. The other set of simulations considered two trucks: original with statutory rigid FUPD and one with e.a. FUPD. The triggering force for the e.a FUPD was 0 kN for both sets of simulation. The resistance force linearly increased until it reached a specified force (for 100 mm deformation) and then it was kept

constant (plateau). All the models in the first set included e.a FUPD with plateau force of 200 kN. The e.a. FUPD in the second test had a plateau force of 250 kN. The conclusion was that the most benefit of using e.a. FUPD was found to be for 75% horizontal overlap especially when the steering unit and towing hooks were not present in the truck front.

An in-depth accident analysis (Krusper and Thomson 2008) showed that the FUPD height could be sensitive to the truck load and a taller FUPD could compensate for vertical variations. A more critical observation was that FUPD cross-beams may be both positioned too low and/or insufficiently stiff to limit cars underriding trucks even when with rigid FUPDs.

From accident and structural analysis of trucks and passenger cars (Krusper and Thomson 2008) it was seen that the vertical overlaps between longitudinals and FUPDs varies. The placement of the FUPD relative to the other truck's parts depends primarily on ground the clearance of a truck's frame which depends on purpose of the truck and placement of its other structural parts. Since, passenger cars are more sensitive to vertical than to horizontal overlaps (Thomson et. al.) these differences cannot be neglected in study of e.a. FUPD performance. Also, the activation force and energy absorption capacity of these systems needed to be further evaluated.

The goal of this study is to extend the previous research and identify the total system performance of the HGV and e.a. FUPD and provide insight into issues relevant for heavy truck design. The study is based on and is continuation of a studies on e.a. FUPDs: accident and structural analysis (Krusper and Thomson 2008) which identified the problems related to FUPDs; investigation of e.a FUPDs theoretical possibilities to absorb energy when interacting with cars under different vertical and horizontal overlaps (Krusper and Thomson 2010); and then comparison was made between the

performance of e.a. FUPDs with 120 mm and 240 mm front surface (Krusper and Thomson 2010).

The performance of e.a. FUPDs of two different heights in interaction with passenger car was investigated when it is installed on truck and not completely free to deform due to its additional interaction with truck. It was found that performance of FUPD is decreased from its theoretical possibilities due to interactions with truck front and passenger car. When the vertical offset between the FUPD and truck frame rails is too small the efficiency of the FUPD is further decreased. Incorporating deformable truck frame elements is only beneficial if the vertical offset between the FUPD and truck frame rails is at least 220 mm. On the other hand stiff truck frame rails have more influence on FUPD performance under different vertical overlaps than the deformable ones.

Methodology

To complement the previous study of the idealized impact of a car and an e.a. FUPD, the total truck and FUPD structure was simulated with impacts of passenger cars. Similar to the previous study, different collision configurations were studied to see how the striking car interacts with the stiffer components of the truck. The results from the previous studies were used to evaluate the difference in e.a. FUPD efficiency between the situation when the truck was not present and when the e.a. FUPD is integrated into truck so both the passenger car and FUPD interact with stiffer parts of the truck. The model of an e.a. FUPD used in the previous study showed good performance with interaction with passenger car. Therefore, eventual poor performance of the FUPD in interaction with passenger car and truck structures can only be a result of additional interactions with truck structures.

The main parameters investigated in this series were: vertical and horizontal alignment of the car and FUPD when it is installed on the truck, vertical distance between the FUPD and rigid truck frame, vertical height (cross-section) of the FUPD, and the influence of deformable truck rails. Part of the simulation series were intended to investigate effects of both impact speed and vehicle mass, but also the energy absorbing element's force levels. Impact speeds of 75 km/h were studied for a mid size (Ford Taurus). A smaller 900 kg (Geo Metro), and a 1330 kg car (Dodge Neon) were used at 56 km/h. These models exhibited weak compartments and were not used for higher impact speeds. They were used to investigate an FUPD activation forces for light vehicles.

Models

All simulations were performed using LS-Dyna (Livermore 2007). Three types of finite element (FE) models were used: passenger cars, e.a. FUPD, and a simplified truck model. In the simulations, the passenger car was the bullet vehicle while the truck was stationary. The ends of e.a. elements of the FUPD are fixed to the front of the truck under its frame rails and they do not move relative to the truck.

The model of the passenger cars are the NCAC derived Taurus, GEO Metro and Dodge Neon models. The Taurus NCAC (2007) model of a 2001 Ford Taurus is somewhat modified to make it more representative of a European car in crash performance against Full Width Rigid Barrier (FWRB) and simplified to decrease calculation time (Thomson et al. 2008). As a reference for modifications, results of impact against rigid barrier for 22 European vehicles performed at NHTSA (National Highway Traffic Safety Administration) were used (Figure 1). The model has been used in the most of simulations for investigation of e.a. FUPD performance. Both the NCAC derived GEO Metro and Dodge Neon models were used to simulate smaller vehicles

impacting the FUPD. These models represent dated (1990's) vehicle designs and were not used to study detailed vehicle response. All car models are shown by Figure 2. Their main longitudinals are highlighted.

The models of the e.a. FUPDs are those used in the previous study (Krusper and Thomson 2010, 2010). The e.a. FUPD model is shown in Figure 3a. The e.a. elements are modeled as springs with 6 degrees of freedom. The spring model has advantages over a real model of FUPD since performance of a real FUPD is limited by its design. The practical example is standard e.a. FUPD used in one of VC-Compat tests which energy absorbing elements were not triggered in the test. The model with spring elements allowed easy setting of triggering force and maximum deformation length. Also, it was easy to tune the force/moment vs displacement/rotation characteristics to 75 kmh^{-1} impact speed and assure some energy absorption by the FUPD for all three horizontal overlaps. The axial triggering force was set to 160 kN (Figure 3b). All forces and moments characteristics are set to linearly increase until reaching a specified value thereafter it remains constant to assure stable deformation of the car hitting the FUPD (Schram et al. 2006). Available deformation distance (displacement) has been chosen to be 300 mm. This displacement corresponds to available space between the front surface of the truck frame and near front suspension mounts measured on three newer trucks listed in the VC-Compat structural database. The vertical size of the FUPD cross beam was varied between 120 to 240 mm. The FUPD crossbeam bending strength was adapted to the dimensions so that the same deformation would be achieved for an identical point load dynamically applied to the FUPD end for both 120 and 240 mm FUPDS (Krusper and Thomson 2010). The mass of the crossbeams were normalized to eliminate any inertial effects between the simulation cases. Material properties for the FUPD beam model were taken from existing Volvo e.a. FUPD beam.

Figure 4 shows the truck model with frame, radiator components, and incorporated e.a. FUPD. The model includes truck components seen in tests performed by Working Group 14 in EEVC (EEVC WG 14 1996). The dimensions for truck rails were taken from VC- Compat truck database. The model for radiator components is based on SCANIA truck models. All other parts under the radiator components were not necessary to model since the stiff FUPD beam does not allow passenger car to travel further than the e.a. elements supports, i.e, in this case, front suspensions. The forward elements of the truck model are deformable except the transparent section of the main frame. This section was varied between rigid (effective stiffness of truck rail) and deformable (proposed modification).

Simulations

All vertical alignments are measured between the car longitudinals and the 120 mm e.a. FUPD (smallest) cross-section and expressed as a percentage relative to the passenger car longitudinals. The vertical offsets between the truck frame rails and FUPD refer to the distance between the FUPD centerline and the lower surface of the truck frame rail. Therefore, different vertical sizes of the cross-beams give different sizes of the contact area between the car and FUPD but also between the truck cooler and FUPD cross-beam. The vertical size of the cross-beam influences also the clearance between the upper surface of the cross-beam and lower surface of the truck frame rails. Vertical alignments were varied from full overlap to 50% percent overlap where two positions of the FUPD were considered: higher and lower relative to car longitudinals. When changing vertical overlap, the whole truck structure with FUPD was moved relative to the car. For the horizontal overlap, three positions were considered in the simulations: full overlap, 75% and 50% relative to the car front end. Finally two stiffnesses of the front part of the truck rails were investigated: rigid and deformable (same material

properties as car longitudinals).

A Geo Metro model was run against the truck model for speeds of 56 and 75 km/h with horizontal overlap of 75% and full vertical overlap. A Dodge Neon model was also run against truck with an impact speed of 56 km/h, 50% horizontal overlap and full vertical overlap.

Simulations performed are given by Tables 1, 2, and 3 together with the previously performed simulations (Krusper and Thomson 2010, 2010) where the Taurus model was run against an e.a. FUPD mounted independent of the truck.

Output Parameters

Since a model of the dummy was not included in the simulations, the intrusions into the occupant compartment and car accelerations were used as the indicator of severity (Delannoy et al. 2005, Thomas 2005). The points on the firewall where the intrusions were measured on the Taurus model (passenger car in further text) are shown in Figure 5.

The points on the two upper rows were considered to belong to the dashboard while the remaining points refer to the footwell area of the firewall. Other output parameters were mostly used to clarify and understand the crash interaction and performance of the component models. For the latter purpose, ride down distance, forces and moments at e.a. deformable elements, amount of energy absorbed by the car, e.a. FUPD and truck, residual, sliding energy and hourglass energy are used.

Results

The amount of hourglass energy developed during the simulations (around 1.3% - less than 6 % of the total energy) and examination of the balance of system energy

components showed that all simulations performed are reliable (Consolazio et al. 2003). The glstat data from two simulations are given in Figure 6.

The influence of the truck architecture on e.a. FUPD performance was investigated by comparing the results from passenger car -to-e.a. FUPD simulations with passenger car -to-rigid frame truck simulations. Figure 7 shows how the deformation patterns of the passenger car changes between the idealized case of the car to FWRB, car-e.a. FUPD, and car-e.a. FUPD when it is included in the truck frame. The sill buckled in all three cases but the deformation was most severe for the car-FWRB impact. An e.a. FUPD offers additional energy absorbing components than the FWRB but Figure 7 shows there is a much smaller interaction surface, with or without the truck frame, when compared to a car-FWRB impact. The least deformation was found for car-FUPD impact when the e.a. FUPD could deform freely. Severe deformations were registered for car– rigid truck frame impacts but they were smaller than in the case of the car-FWRB impact. The efficiency of the e.a. FUPD was seen to decrease due to car interactions with truck structurs and also interactions between the truck cooler and FUPD.

Intrusions for the car-to-FUPD are compared to the intrusions for the close FUPD/frame placement in a HGV (frame – FUPD offset of 160 mm) (Figure 8). All intrusions are normalized to the average intrusion of the entire firewall for the car-to-FWRB impact simulations. A distinction is made between intrusions registered at dashboard and footwell. In general for FUPD impacts, the intrusions at the dashboard are higher than those registered at the firewall while the opposite occurs for the car-to-FWRB impacts.

The intrusions for car-to-rigid frame truck impacts (right side of Figure 8) are higher than those registered for car-to-FUPD impacts (left side of Figure 8). While an

isolated FUPD of 240 mm (larger FUPD – black lines) shows better performance for car-to-FUPD compared to a 120 mm FUPD (smaller FUPD - grey lines), this advantage is less obvious or disappears when the rigid frame rails are closely placed to the FUPD. For the same vertical overlap and different horizontal overlaps there is more variation in intrusions when the truck is present. Also intrusions are increasing with smaller horizontal overlap. As shown in Figure 6, the rigid frame rails contact the upper front structures of the car and limit the stroke of the e.a. FUPD. The combination of these actions results in higher intrusions as more energy must be absorbed by the car than in the FUPD case only.

The intrusions at the car dashboard for car-to-FUPD impact when a FUPD of 120 mm is placed higher exceed intrusions registered for car-to-FWRB impact in Figure 8. This is an overriding position of the FUPD and is the worst loading case for the car. It is also expected that higher intrusions will be registered for car-to-rigid frame truck when a FUPD is placed higher, relative to the car, regardless of its cross-beam height since the upper part of car front is loaded not only by FUPD but also by stiffer truck structures. Inspection of the simulations confirmed that the truck parts partly prevent backward movement of the FUPD cross beam and therefore limits full deformation of e.a. elements.

It was noticed in previous studies that the bending of the idealized FUPD cross-beam for lower horizontal overlaps allows rotation of the car which limits deformations of the car (Krusper and Thomson 2010). Some of the original impact energy remains in the post impact kinetic energy and is not directed into structural deformation energy. The reduced deformation of the FUPD cross-beam for car-to-rigid frame truck is also prevented by the stiffer truck parts and the car continues to translate instead of rotating, resulting in more car deformations.

Acceleration vs. displacement curves (Figure 9) are similar for car-to-FUPD and car-to-rigid frame truck when a FUPD of 120 mm is used. Somewhat earlier but higher acceleration peaks can be seen for car-to-rigid frame truck cases since the hard truck parts deforms higher parts of the car front and partially softens the impact when deformation of e.a. elements stopped. The acceleration peaks for the car-rigid frame truck correspond to the moment when the car impacts the truck's rigid frame elements while the acceleration peak for the car-FUPD impact occur when the forces in e.a. elements reach their maximum and the car front end stops deforming. There is no significant difference in acceleration vs displacement curves for the FUPDs.

A distribution of absorbed energy for these cases is shown by Figure 10. When the truck structure is present, the energy absorbed by a FUPD decreases from 30 to 14% and from 32 to 12% for FUPD sizes of 120 and 240 mm respectively.

The influence of the stiffness of truck frame rails and the distance between FUPD centerline and truck frame's lower surface on intrusions of the car firewall is shown by Figures 11 (rigid frames rails) and Figure 12 (deformable frame rails). The reference intrusion in all cases is the FWRB load case. Even for deformable truck rails, intrusions are higher for the dashboard than for the footwell. Three distances between the centerline of the FUPD and the lower surface of the truck frame rails are presented: 160, 220 and 280 mm. Regardless of the distance between the centerline of the e.a. FUPD and the lower surface of the truck frame rails, less intrusions were registered when the car was run against truck with deformable rails for the same crash configuration. On the other hand, regardless the stiffness of the frame, the worst results are obtained for close FUPD/frame placement (frame – FUPD offset of 160 mm).

An e.a. FUPD exhibits the best performance for full horizontal overlap. The intrusions for both, 75 and 100% horizontal overlaps, are less when the FUPD of 240 mm is used but it is not always the case for 50% overlap.

When the FUPD is placed lower or fully overlaps vertically with the car longitudinals, the deformable frame causes less intrusion. Even for smaller overlaps and higher placed truck frame (offset 280 mm), the intrusions are higher than in the idealized case, i.e. when the truck is not present (Figure 13, left). The acceleration vs displacement curve shows a very sharp peak at the end for the case when only the FUPD interacts with the car (Figure 13, right). It corresponds to the impact with FUPD supports. This impact is not present in car-to-truck cases.

The advantage of having a deformable frame is also visible for the offset of 220 mm. The center figures in Figure 12 (deformable frame) can be compared to those in Figure 11 (rigid frame). Here, a smaller offset caused more overlap between the car and the truck cooler as well as the deformable truck frame. The higher overlap was sufficient to deform the frame and cooler. The deformation gave space for FUPD deformation allowing e.a. elements to deform further. When looking at acceleration vs displacement curves for the simulated cases (Figures 14 and 15), it can be seen that here the advantage of having deformable truck frame rails is highest for 75% horizontal overlap but still depends on the offset.

Figure 16 shows that energy absorption is more influenced by the stiffness of truck frame rails in the case of higher FUPD. The difference in energies absorbed by the car and FUPD is relatively high for impact into truck with deformable rails and for the two different heights of FUPDs. Intrusions differences for the rigid truck rails are not so obvious (Figure 12). Acceleration vs displacement curves show differences in the

acceleration values for the two cases. The acceleration is higher for smaller FUPD and implies higher impact force.

Figure 17 and 18 shows that energy absorption is less influenced by the offset for deformable truck frame rails and FUPD of 240 mm than for the same cases but with rigid truck frames. Also for the cases with rigid truck frame, the difference in energy absorption is less if FUPD of 120 mm is used. The lowest amount of energy absorbed by the FUPD is around 38 kJ and refers to higher FUPD, 75% horizontal overlap and rigid truck frame rails with offset of 160 mm. The highest value registered is 97 kJ and refers also to a larger FUPD, but deformable truck frame rails, 50% horizontal and 50% vertical overlap and lower placed FUPD relative to car longitudinals.

Finally, maximum force and moments resultants registered are found for different cases. The maximum force in the axial direction of e.a. element has reached the maximum possible resistant force of the e.a. elements (Figure 4), while forces in other directions and moments are under the highest values specified for the elements. Still the displacements of the free end of the e.a. elements in lateral and vertical directions are relatively small.

A concern for the FUP designs was that the activation force and subsequent force-deflection curve for the FUPD may be too high for a smaller vehicle. As seen in Figure 12, the forces of car-barrier and car-FUP impacts lie in the same corridor up to 20 ms when the load reaches 200 kN. The Ford Taurus - FWRB data is also plotted for reference.

The Geo Metro and Dodge Neon showed maximum wall loads of 500 kN in the FWRB configuration at 56 km/h. The rigid wall impacts at 56 km/h are plotted on the same figure as the car to HGV and FUPD impacts. Both small vehicles began to exhibit compartment deformations at around 20 ms in this case and are about 250 kN in the

FWRB case. Although their peak forces exceeded 450 kN, the compartment was not stable enough for a 75 km/h impact.

The FUP springs were activated in all the simulations with lighter vehicles and were compressed to at least 2/3 of their original length indicating that the all masses of the simulated vehicle were able to activate and deform the FUPD. At 56 km/h, compartment deformations were acceptable but this was not the case for higher speeds. For reference, the Taurus exhibited initial signs of compartment deformation in a FWRB when the wall forces were estimated at 650kN (Figure 19).

Discussion

From the previous study it was found that the stiffness of the e.a. FUPD cross-beam and the axial triggering force of the e.a. elements and vertical height of the cross-beam cross section are the factors influencing efficiency of the e.a. FUPD. The research was based on the impact simulations between car and e.a. FUPD. Since, the FUPD beam interacts directly with passenger car front structures, stiff beams are able to transfer impact force to energy absorbing elements and at the same time keeps the contact surface spread over the car front preventing a fork effect. Also, It was shown that FUPD with higher beam cross section provides better structural interaction with the car, resulting in higher energy absorption by the FUPD. The energy absorbed by the FUPD for all cases varied from 65 to 115 kJ depending on vertical and horizontal overlap but also on height of front beam surface. After finding an adequate stiffness, and triggering force, e.a. absorbing FUPD of two cross-beam cross-section heights were found less severe to the impacting car than FWRB. It shows that the energy absorbed by the e.a. FUPD influenced the impact in more positive way than the reduction of the contact surface influenced it in negative way. In all cases there was a trend of intrusion reduction as

horizontal overlap decreased under 75% implying that e.a. FUPD makes car crash more predictable in comparison to car to car crashes (Thomson et al., 2008). When the car impacts e.a. FUPD the intrusions are always higher at the dashboard than at the footwell while the opposite stands for the impact against FWRB. The FWRB forces deformation of the whole car front while e.a. FUPD interacts directly almost only with longitudinals of the car. The result is that the longitudinal bends up and pushes the dashboard on reward. This is most obvious for the case when the FUPD is placed higher relative to the longitudinal. However, intrusions at the car firewall were always less after the car impacted the e.a. FUPD than after impact with the FWRB. Only when the smaller FUPD was placed higher than the longituinals and for 75% and 50% horizontal overlap did the intrusions at the dashboard exceeded the intrusions registered for the impact against FWRB. Therefore, the model chosen for e.a. FUPD can be considered efficient in reducing the severity of frontal crashes with passenger cars. But that was an idealized case where the e.a. elements of the FUPD could deform freely and its efficiency depended only on its structural interaction with passenger car. The question is if it is possible to keep the same ability of e.a. FUPD to absorb the energy even when it is installed at the truck and how the ability varies depending on FUPD placement at the truck relative to car's longitudinals and truck's rails.

When integrated into truck a structure, the e.a. FUPD interacts not only with passenger car front but also with the truck structure. The contact area between the car front and its target is increased but the truck structure restricted the deformation of the FUPD e.a. elements. In the car-truck simulations the offset between the truck frame rails and FUPD was varied. These offsets were combined with different vertical and horizontal overlaps between the car longitudinals and the FUPD. Also FUPD with higher and smaller cross-beam cross sections were used and two different stiffnesses of

the truck rails were considered. Since, the higher placed e.a. FUPD does not give desirable results even for the idealized case it has been concluded that the higher placed FUPD together with truck frame rails will cause even worse results. Therefore, less attention is paid on these cases and only few simulations were run with higher placed FUPD.

In general, an e.a. FUPD performed better when the truck structures were not present since the e.a. elements could deform freely. The truck structure interacted with the car and the FUPD contacted the truck cooling system and frame rails. Depending on the offset between the FUPD centerline and lower surface of the truck frame, different portions of the FUPD and truck cooling system overlapped. In some cases this overlap facilitated deformation of the truck frame and radiator (case of offset 220 mm). The deformable frame allowed rearward movement of the radiator but also took up some energy through deformations. The energy absorbed by the truck was small in all cases (up to 6 kJ) for deformable truck frame but the energy absorbed by the FUPD was much higher when compared to cases with rigid truck frame. It can be concluded that the ability of deformable truck frame rails to take up energy is of less importance than the fact that a deformable frame allows further backward movement of the FUPD. However, the energy absorbing capabilities of FUPD could not be fully used. The reduction in FUPD energy dissipation is accompanied by a corresponding increase in energy absorbed by the car in both cases. Deformation of the higher FUPD is more restricted by contact with the truck structure since it builds a larger contact area with truck cooler. As a result it influences the amount of energy needed to be absorbed by the car making larger differences in energy absorbed by the car and higher FUPD than energy absorbed by the car and smaller FUPD.

The intrusions for both 75% and 100% horizontal overlaps are less when the FUPD of 240 mm is used but it is not always the case for 50% overlap. For 50% horizontal overlap the outcome is less predictable. For the case of 280 mm frame – FUPD offset and higher placed FUPD the frame is placed sufficiently high to not interact with the car and FUPDs behaviour is similar to one when the truck is not presented. Still, the truck cooler is at the level of the FUPD and prevents the e.a. elements to deform completely. Since the truck frame is not deformed at all for both cases it is not expected to see a big difference in intrusions even if the frame was rigid.

Acceleration was slightly more spread over displacement when the truck is present. On the other hand, the stopping distance was generally shorter and accelerations higher for these cases in comparison to idealized situations (car against e.a. FUPD only). Still better results were obtained for the deformable frame than for the rigid frame, especially for 75% horizontal overlap.

In the cases with rigid truck frame benefit advantages of having larger FUPD almost disappeared, and became only beneficial again when deformable truck frame was used. Larger FUPDs in combination with deformable truck rails gives lower intrusions, lower acceleration and less variation in these values than smaller FUPD. Smaller FUPD give less variation of intrusions for the rigid truck frame than when the larger FUPD was used in combination with the same rigid frame.

The highest force and moment resultant together with maximum displacement of free ends of e.a. elements in lateral and vertical directions showed that prescribed spring characteristics at the FUPD model were sufficient to assure stable deformation of the car. These values provide design input for the physical structures used in e.a. FUPD.

Maximum deformation of e.a. elements in the impact direction was 270 mm and implies that available stroke of 300 mm could not be efficiently used. Since, the

maximum resistance force of e.a. elements in traveling direction was reached the only reason that the available deformation distance could not be used is that the FUPD movement was restricted by integrated truck structures.

Based on the longitudinal FUPD spring forces of 284 kN used in these simulations, future small vehicles should have compartment strengths allowing at least 350-400 kN if these spring stiffnesses are to be considered. Current compatibility research is promoting stronger small car compartments and 350-400kN is the recommendation from the VC-Compat (2007) project**.**

Conclusions

Vehicle collisions with different e.a. FUPD geometries and configurations mounted in trucks were investigated for both vertical and horizontal offset conditions. When the FUPD is mounted on the truck with a rigid frame, the clear advantage of having larger (240 mm) FUPD disappears. A larger idealized FUPD could provide better contact and energy dissipation performance than a 120 mm FUPD. The main issue that arises is that when a FUPD was mounted on a truck, the frame rails and truck cooler interfered with the FUPD performance. Contacts of the car to stiffer truck structures and FUPD contact with the cooling system of the truck were observed. Small frame-FUPD offset is undesirable regardless the stiffness of the truck frames, while the advantage of having deformable truck frames increases with the FUPD-frame offset and at least 220mm is needed. The ability of deformable truck frame rails to take up energy is less influencing on crash outcome than the fact that deformable frame allows further backward movement of the FUPD than it is case for the rigid truck frame rails. In combination with deformable truck frame rails, larger FUPD shows again better performance than the smaller one.

Acknowledgments

The authors would like to thank the Vinnova Program for Vehicle research (PFF) for enabling this work, project partners (VCC, Saab Automobile, Volvo 3P, Scania, and Autoliv Research) for their cooperation and NCAC for sharing their models with the rest of the world.

References

Delannoy P, Martin T, Castaing P. 2005. Comparative evaluation of frontal offset tests on control self and partner protection. Proceeedings of 19th International Technical Conference on the Enhanced Safety Vehicles, paper No. 05-0010.

EEVC WG 14, European Enhanced Vehicle-safety Committee Working Group 14. 1996. Estimation of influence of rigid FUPDs on injuries to car occupants; Benefits of e.a. FUPs for trucks compared with rigid devices. Report.

European Experimental Vehicle Committee, (Now European Enhanced Vehicle-safety Committee). 1996. The validation of EEVC Frontal Impact Procedure. Proceedings of 15th International Technical Conference on the Enhanced Safety of Vehicles. Paper 96-S3-O-28.

Forsman, L. 2002. Compatibility in Truck to Car Frontal Impacts. 7th International Symposium on Heavy Vehicles Weights & Dimensions. Delft (Netherlands)

Gwehenberger J, Bende J, Knight I, Klootwijk C. 2003. Collection of Existing Indepth Accident Cases and Prediction of Benefit on Having Front and Rear Underrun Protection. VC-Compat. Task 2.7/2.8. European Commission Project N° GRD2/2001/50083.

Krusper A, Thomson R. 2008. Compatibility between Heavy Goods Vehicles and Passenger Cars: Structural Interaction Analysis and In-depth Accident Analysis. Proceedings of International Conference on Heavy Vehicles, Paper N° 25. Paris (France)

Krusper A, Thomson R. 2010. Energy-absorbing FUPDs and their interaction with fronts of passenger cars. International Journal of Crashworthiness, 15: 6, 635 — 647

Krusper A, Thomson R. 2010. Crash performance of front underrun protective device with a passenger car under different crash configurations – Results of finite element method based simulations. Department of Applied Mechanics. Chalmers University of Technology.Research report 2010:07. Gothenburg (Sweden).

Livermore Software Technology Corp. 2007. LS-DYNA® keyword user's manual-version 971.

[NCAC] National Crash Analysis Center [Internet]. 2001 Ford Taurus; [downloaded 2007 May 22]. Available from: http://www.ncac.gwu.edu/.

[NHTSA] National Highway Traffic Safety Administration. 1998. Trends in large truck crashes. National Technical Information Services. DOT-HS-808-690. Springfield. Virginia (USA).

Rechnitzer G. 1993. Truck involved crash study, fatal and injury crashes of cars and other road users with the front and sides of heavy vehicles. A research project for VIC ROADS Road Safety Division. Report N° 35.

Schram R, Leneman F J W, de Coo P J A, van der Zweep C D. 2006. Report detailing reference baselines to evaluate underrun guard test procedure(s) to be proposed in WP9. Improvement of vehicle crash compatibility through the development of crash test procedures (VC-Compat). Deliverable N° D14. Project N°: GRD2-2001-50083.

Schram R, Leneman F J W, van der Zweep C D, Wismans J S H M, Witteman W J. 2006. Assessment criteria for assessing energy-absorbing front underrun protection on trucks. International Journal of Crashworthiness, 11: 6, 597 — 604.

Schäfer R, Schepers A, Assing K, otte D, Nehmzow J, Faerber E, Adalian C, Cocoual M, Zac R, Césari D, Aparicio F, Páez F J, van Kampen B. 1999. WP2 Accident Analysis. Report for the European Commission DGVII. Volume 3. Contract N°: R0-97-SC.1064

Thomas GE. 2005. Compatibility and structural interaction in passenger vehicle collisions. protection on trucks. Faculty of Engineering, RMIT University. Ph.D. Thesis. Melbourne (Australia).

Thomson R, Krusper A, Avramov A, Rachid K. 2008. The role of vehicle design on structural interaction. International Crashworthiness Conference. Kyoto (Japan).

[VC-Compat] Vehicle Crash Compatibility]. 2007. Vehicle Crash Compatibility through the Development of Crash Test Procedures. Final Technical Report. European Commission Project N°: GRD2/2001/50083.

Table 1. Taurus against e.a. FUPD (speed 75 km/h) – performed in previous work (Krusper and Thomson 2010)

Table 2. Taurus against truck with rigid frame rails (speed 75 km/h)

Table 3. Taurus against truck with deformable frame rails (speed 75 km/h)

Table 4. Maximum force and moment resultants at e.a. elements and maximum displacement of free ends of e.a. elements

Table 1. Taurus against e.a FUPD (speed 75 km/h)-) performed in previous work (Krusper and Thomson 2010)

No.	FUPD height [mm]	Overlap Horizontal [%]	Overlap Vertical [%]	FUPD position relative to car long..	No.	FUPD height [mm]	Overlap Horizontal [%]	Overlap Vertical [%]	FUPD position relative to car long.
1	120	100	50	Higher	10	240	100	50	Higher
2	120	100	100	-	11	240	100	100	-
3	120	100	50	Lower	12	240	100	50	Lower
4	120	75	50	Higher	13	240	75	50	Higher
5	120	75	100	-	14	240	75	100	-
6	120	75	50	Lower	15	240	75	50	Lower
7	120	50	50	Higher	16	240	50	50	Higher
8	120	50	100	-	17	240	50	100	-
9	120	50	50	Lower	18	240	50	50	Lower

Table 2. Taurus against truck with rigid frame rails (speed 75 km/h)

No.	Frame rails – FUPD offset [mm]	FUPD height [mm]	Overlap Horizontal [%]	Overlap Vertical [%]	FUPD position relative to car long.	No.	Frame rails – FUPD offset [mm]	FUPD height [mm]	Overlap Horizontal [%]	Overlap Vertical [%]	FUPD position relative to car long.
1	160	120	100	100	-	12	220	120	75	50	Lower
2	160	120	75	100	-	13	220	240	75	50	Higher
3	160	120	75	50	Lower	14	220	240	75	100	-
4	160	120	50	100	-	15	220	240	75	50	Lower
5	160	120	50	50	Lower	16	280	120	75	100	-
6	160	240	100	100	-	17	280	120	75	50	Lower
7	160	240	75	100	-	18	280	120	50	50	Lower
8	160	240	75	50	Lower	19	280	240	75	100	-
9	160	240	50	100	-	20	280	240	75	50	Lower
10	160	240	50	50	Lower	21	280	240	50	50	Lower
11	220	120	75	100	-						

Table 3. Taurus against truck with deformable frame rails (speed 75 km/h)

No.	Frame rails – FUPD offset [mm]	FUPD height [mm]	Overlap Horizontal [%]	Overlap Vertical [%]	FUPD position relative to car long	No.	Frame rails – FUPD offset [mm]	FUPD height [mm]	Overlap Horizontal [%]	Overlap Vertical [%]	FUPD position relative to car long.
1	160	120	100	100	-	14	220	120	50	50	Lower
2	160	120	75	100	-	15	220	240	100	50	Higher
3	160	120	75	50	Lower	16	220	240	75	50	Higher
4	160	120	50	100	-	17	220	240	75	100	-
5	160	120	50	50	Lower	18	220	240	75	50	Lower
6	160	240	100	100	-	19	220	240	50	50	Higher
7	160	240	75	100		20	280	120	75	50	Lower
8	160	240	75	50	Lower	21	280	120	50	50	Higher
9	160	240	50	100	-	22	280	120	50	50	Lower
10	160	240	50	50	Lower	23	280	240	100	100	-
11	220	120	100	100	-	24	280	240	75	100	-
12	220	120	75	100	-	25	280	240	50	50	Higher
13	220	120	75	50	Lower	26	280	240	50	50	Lower

Table 4. Maximum force and moment resultants at e.a. elements and maximum displacement of free ends of e.a. elements

		FUPD side	Value	Simulation
Max force resultant[kN]	Fr	Left	284	FUPD120 H75% V50%Lower, Offset 220mm, TrR
	Fs	Left	121	FUPD120 H75% V50%Lower, Offset 220mm, TrR
	Ft	Right	96	FUPD120 H75% V50%Lower, Offset 220mm, TrD
Max moment resultant [kNm]	Mr	Left	6	FUPD120 H75% V50%Lower, Offset 220mm, TrR
	Ms	Right	17	FUPD120 H75% V50%Lower, Offset 220mm, TrR
	Mt	Right	11	FUPD240 H50% V50%Higher ,Offset 220mm, TrD
Max displacement [mm]	X	Left	270	FUPD240 H50% V50%Higher, Offset 280mm, TrD
	Y	Right	38	FUPD120 H75% V50Lower, Offset 220mm, TrD
	Z	Right	33	FUPD240 H50% V50%Higher ,Offset 220mm, TrD

Figure 1. Acceleration vs time (left) and rigid wall force vs displacement from rigid barrier test of 22 European vehicles were used as a reference for modification of Taurus model used in the simulations.

Figure 2. FE models of passenger cars.

Figure 3. Model of simplified e.a. FUPD: (a) e.a. FUPD consisting of FUPD cross-beam and FUPD e.a. elements (modelled as springs) and (b) force/moment vs displacement/rotation characteristics of the e.a. elements (springs).

Figure 4. Truck model with incorporated e.a. FUPD.

Figure 5. Points at firewall where intrusions are measured.

Figure 6. Calculated energies for two simulations

Figure 7. Vehicle deformation in three different simulation cases.

Figure 8. Intrusions registered for car- e.a. FUPD (left column) and car-rigid frame truck (right column) impacts. The upper row refers to dashboard intrusions and the lower one to footwell intrusions.

Figure 9. Acceleration vs. displacement curve for full vertical overlap and different horizontal overlaps for car-FUPD (left column) and car-rigid truck.

Figure 10. An energy absorption for car-FUPD and car-rigid frame truck impacts (160 mm frame-FUPD offset) under 75% horizontal and 100% vertical overlaps.

Figure 11. Calculated intrusions of the dashboard and footwell of the car impacting the truck with rigid frame rails

Figure 12. Calculated intrusions of the dashboard and footwell of the car impacting the truck with deformable frame rails

Figure 13. Energy absorption (left) and acceleration - vs. displacement curves (right) for car—rigid frame truck (TrR), car-deformable frame truck (TrD) and car-FUPD impacts when FUPD of 240 mm is used. The horizontal overlap is 50% and vertical overlap is 50% when the FUPD is placed lower relative to the longitudinals.

Figure 14. Acceleration vs displacement curves for the car impacting the truck with rigid frame rails under different horizontal and vertical overlaps.

Figure 15. Acceleration vs displacement curves for the car impacting the truck with deformable frame rails under different horizontal and vertical overlaps.

Figure 16. Comparison between energy distributions for FUPD120 and FUPD240 mounted on trucks with rigid or deformable frame rails.

Figure 17. Comparison of energy distributions for different offsets for a FUPD of 120 mm cross-section mm for rigid and deformable truck frame rails.

Figure 18. Comparison of energy distributions for different offsets for a FUPD of 240 mm cross-section mm for rigid and deformable truck frame rails.

Figure 19. . Frontal forces in 56 km/h impacts for rigid wall and 75% horizontal overlap car-truck/FUPD collisions.

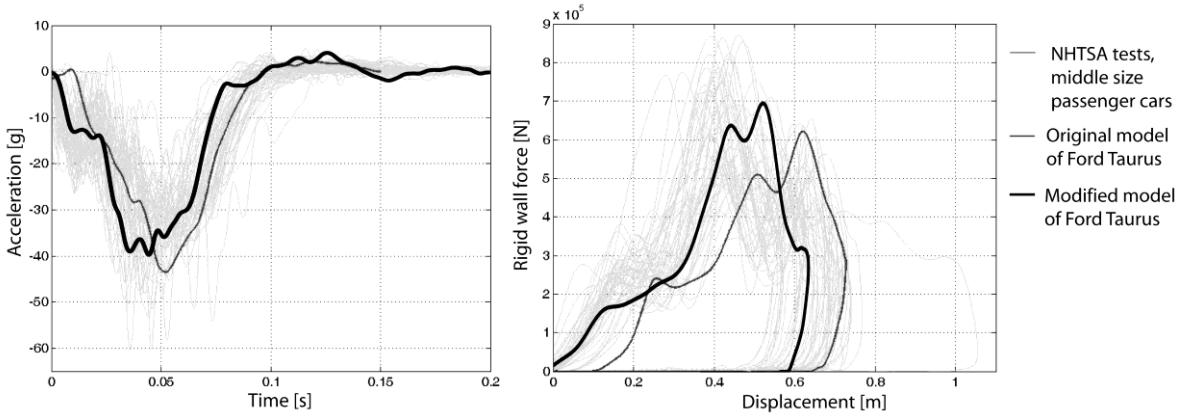

Figure 1

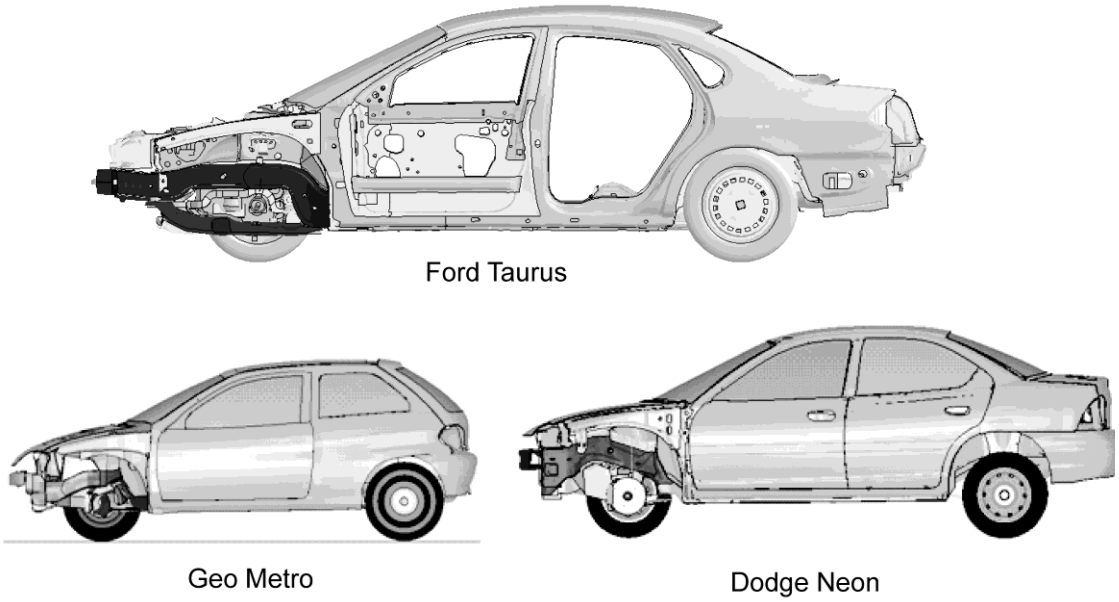

Figure 2

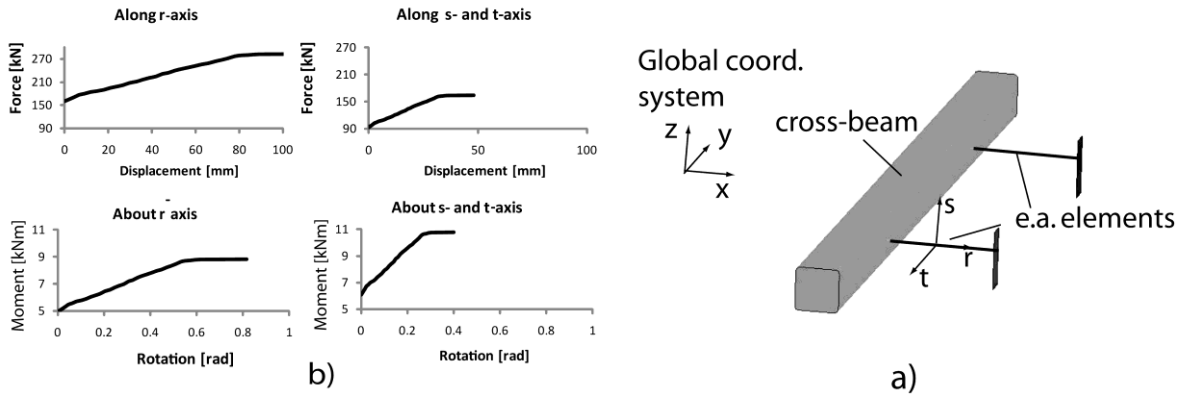

Figure 3

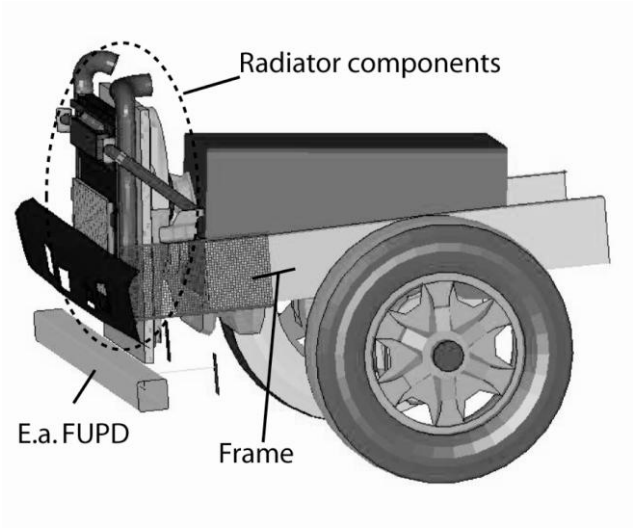

Figure 4

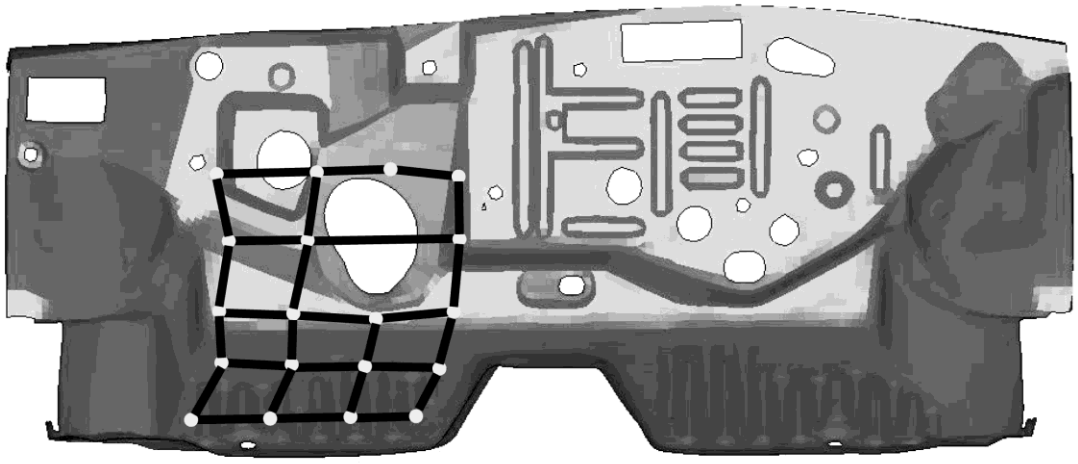

Figure 5

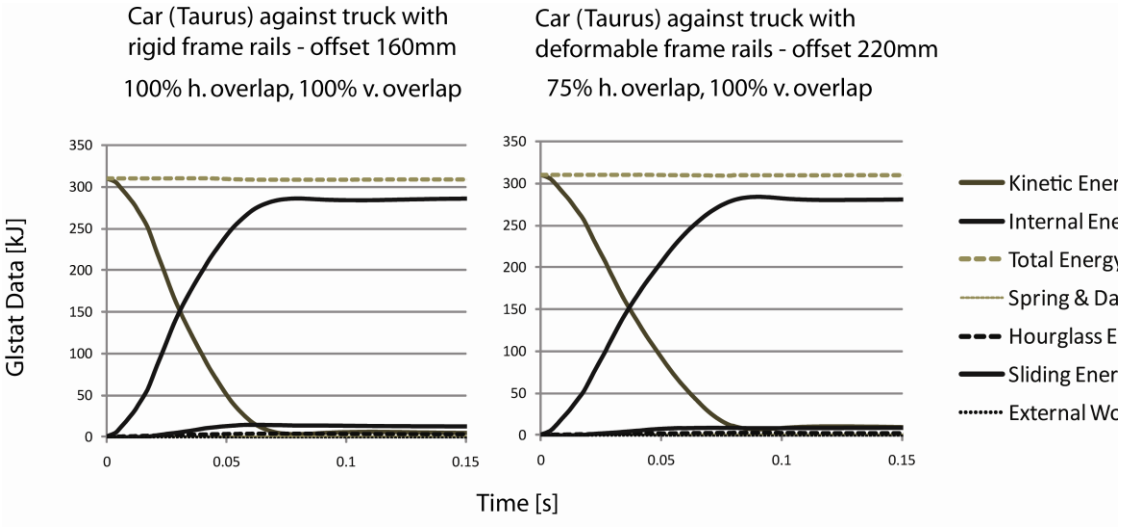

Figure 6

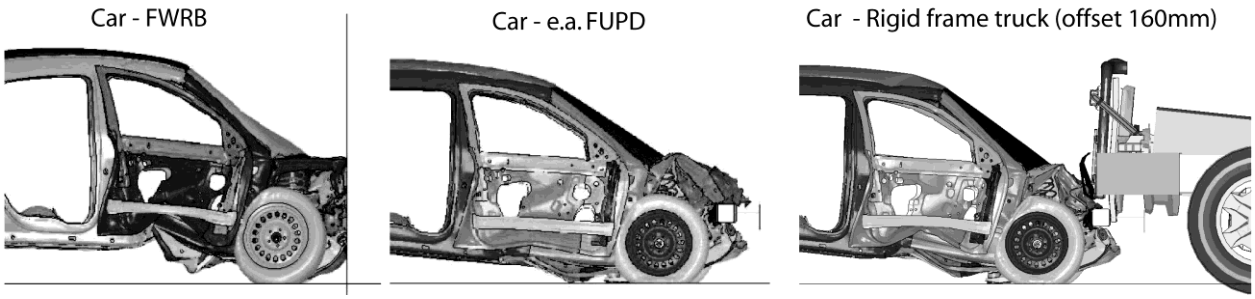

Figure 7

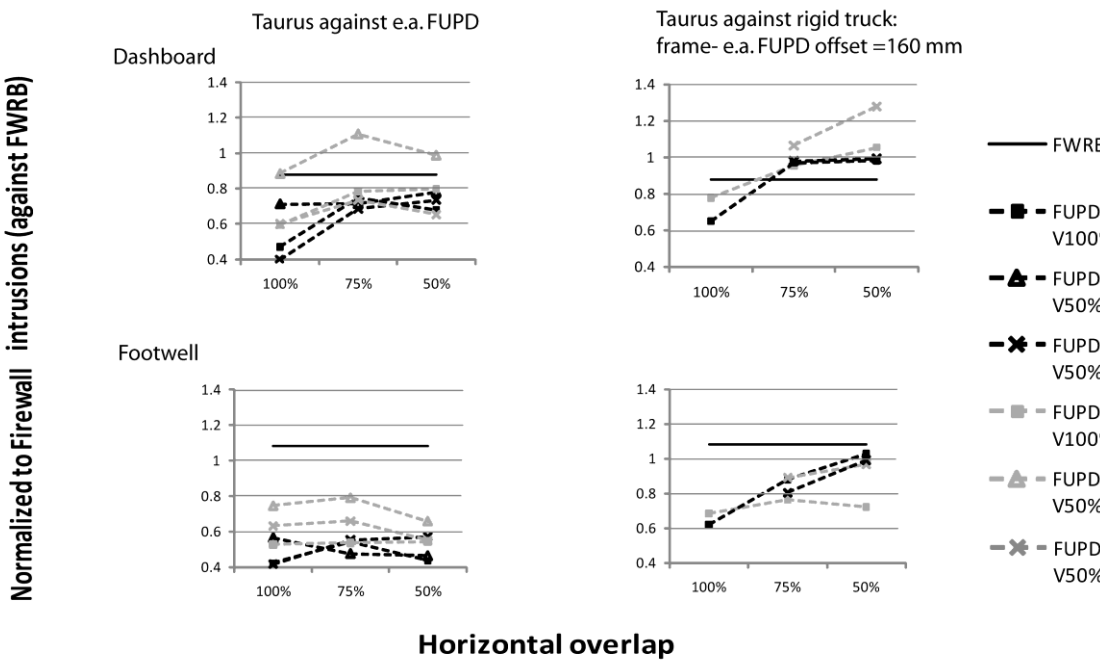

Figure 8

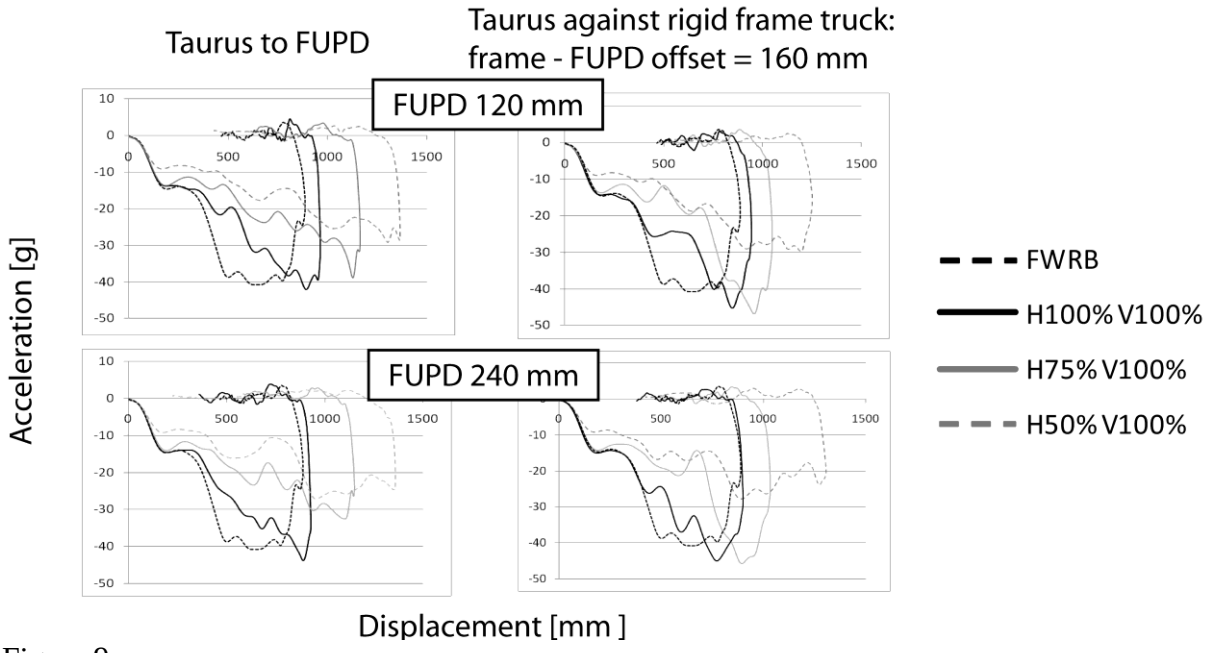

Figure 9

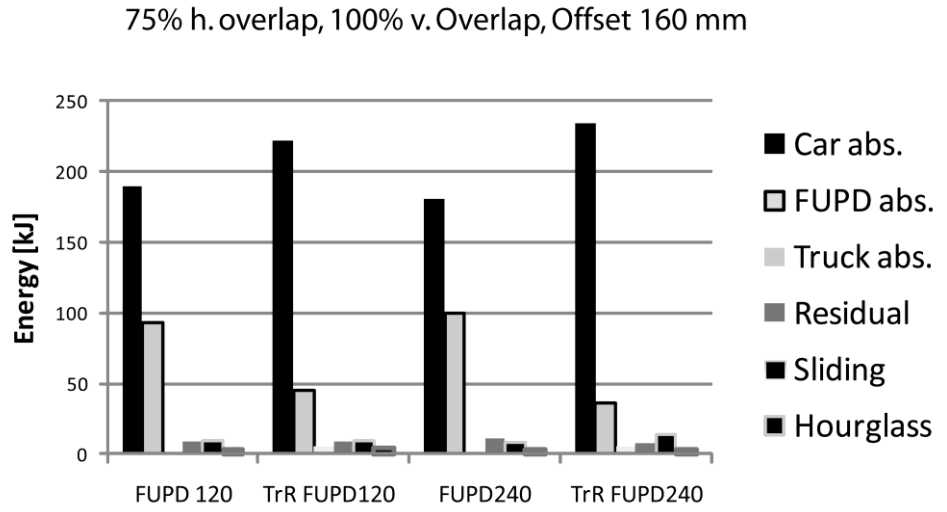

Figure 10

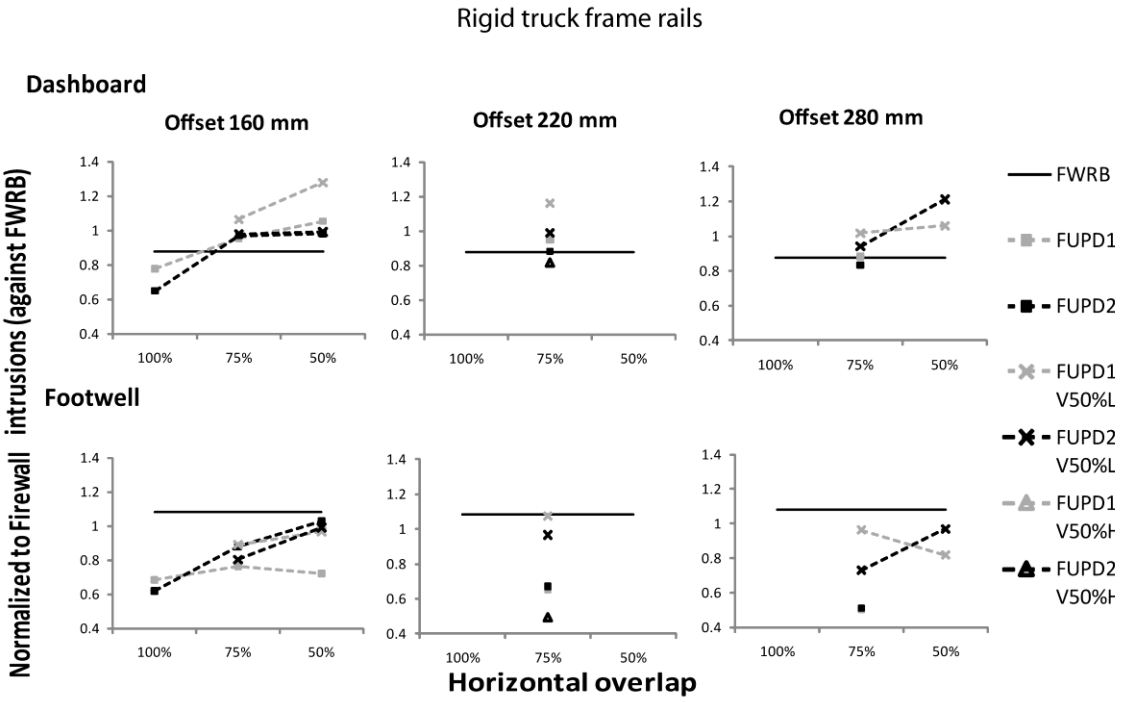

Figure 11

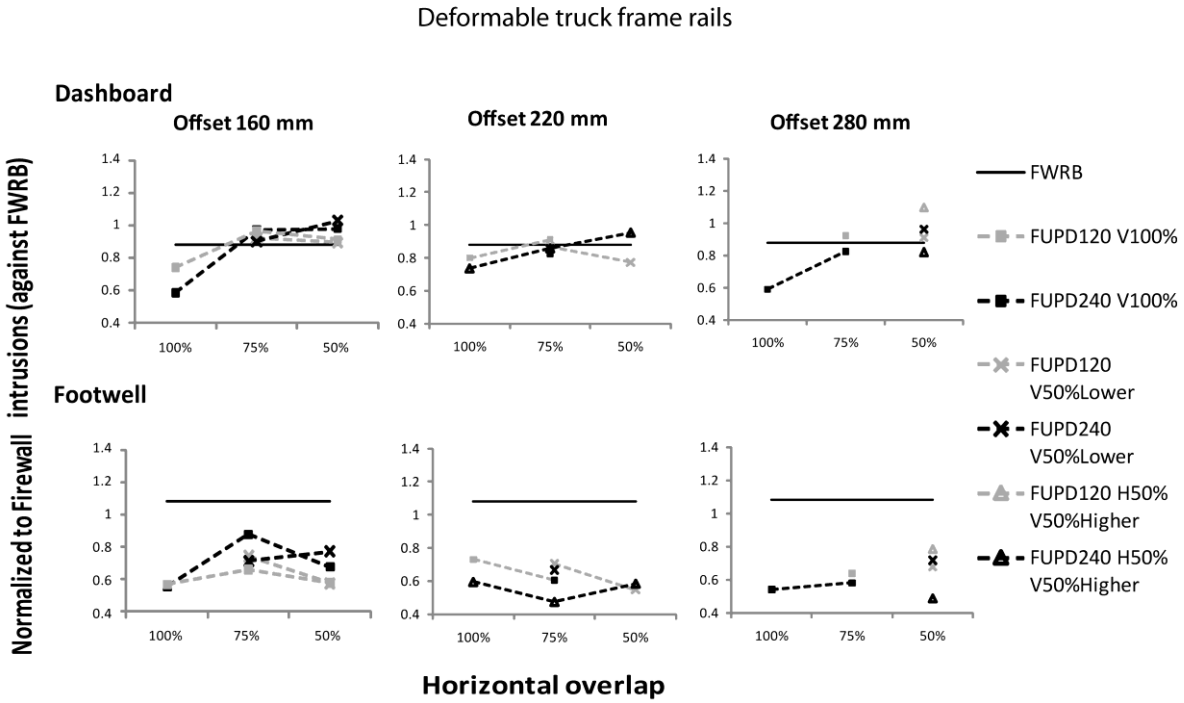

Figure 12

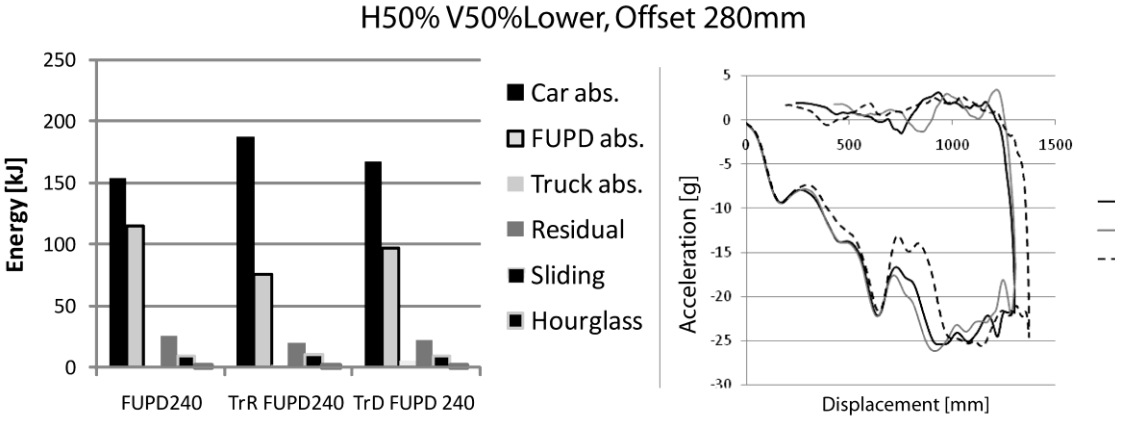

Figure 13

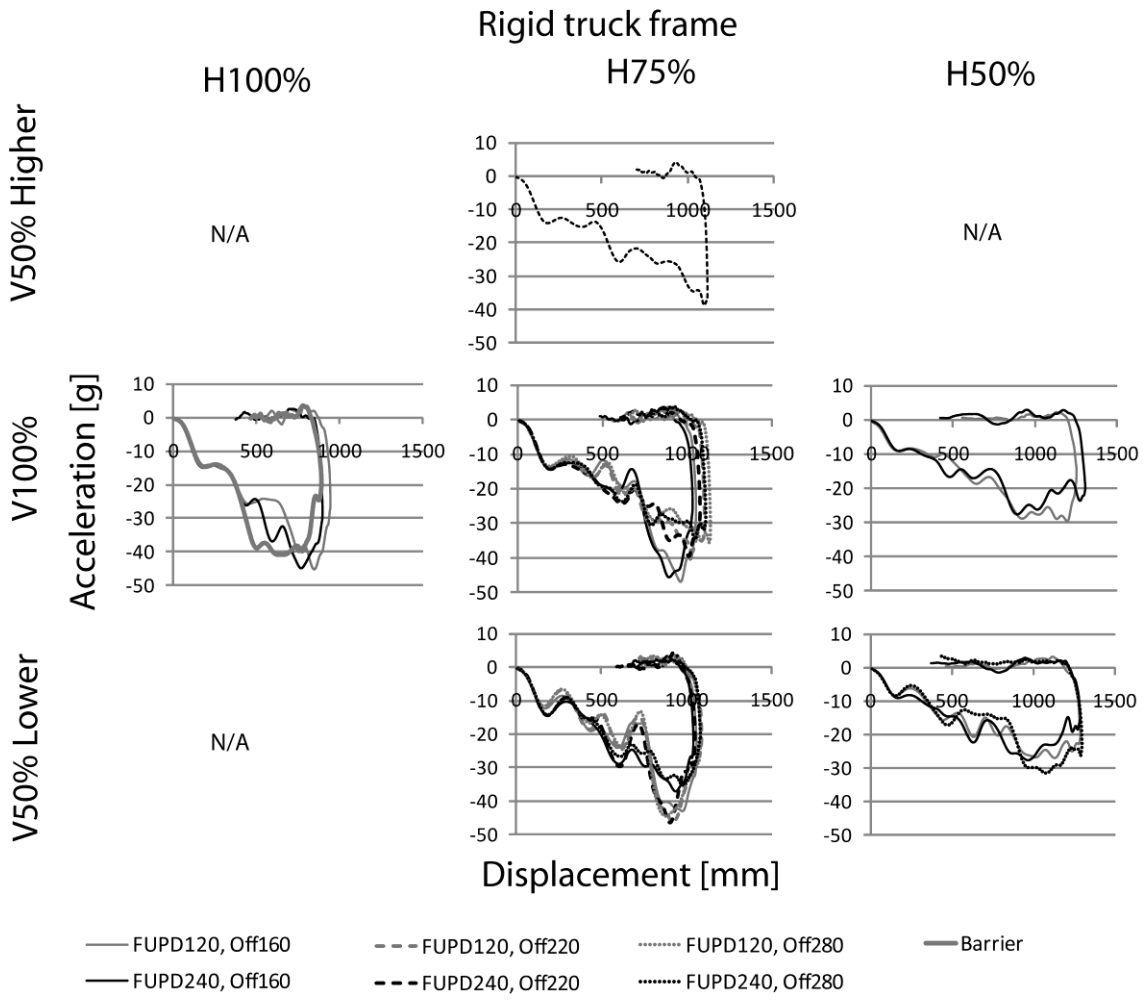
Rigid truck frame
H100%
H75%
H50%
V50% Higher
V100%
V50% Lower
N/A
N/A
N/A
Acceleration [g]
Displacement [mm]
FUPD120, Off160
FUPD120, Off220
FUPD120, Off280
Barrier
FUPD240, Off160
FUPD240, Off220
FUPD240, Off280

Figure 14

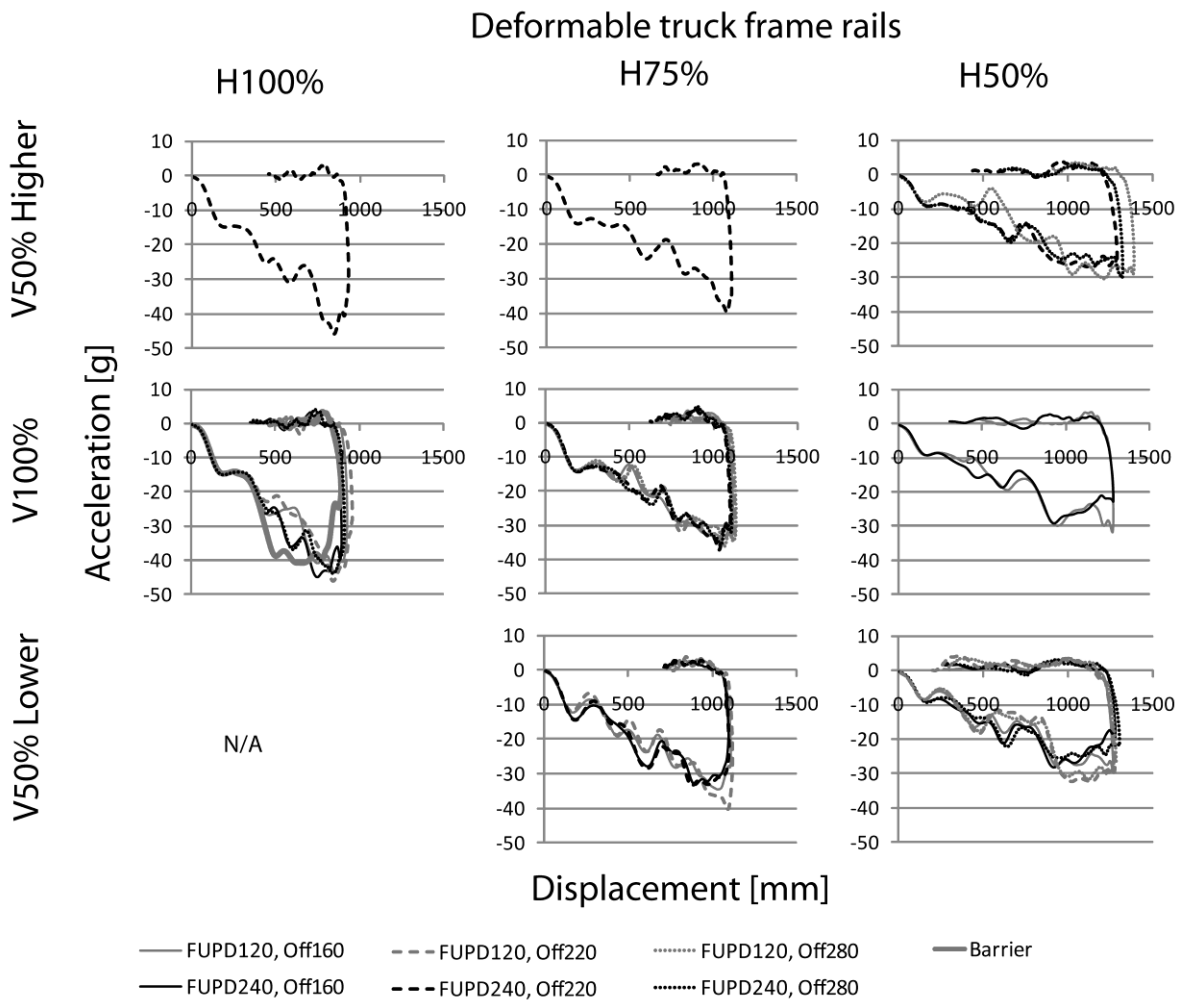

Figure 15

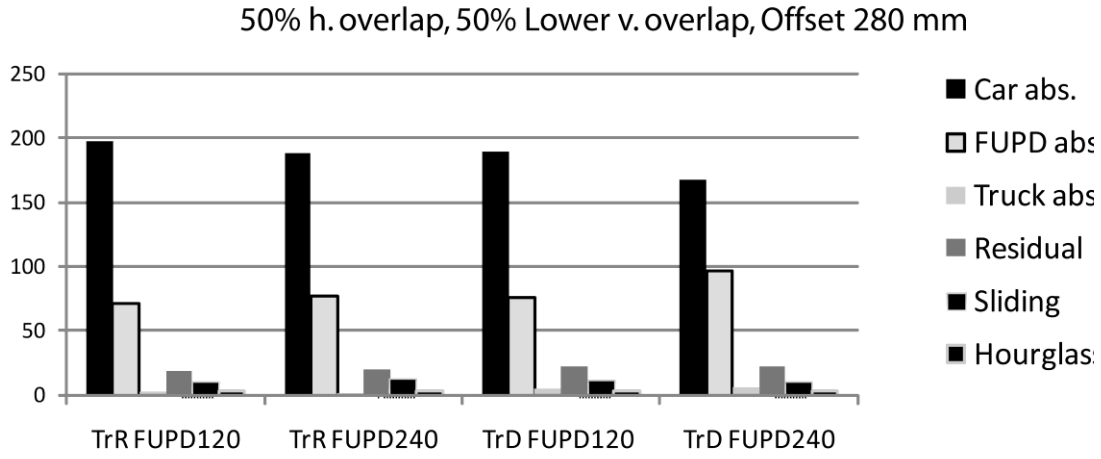

Figure 16

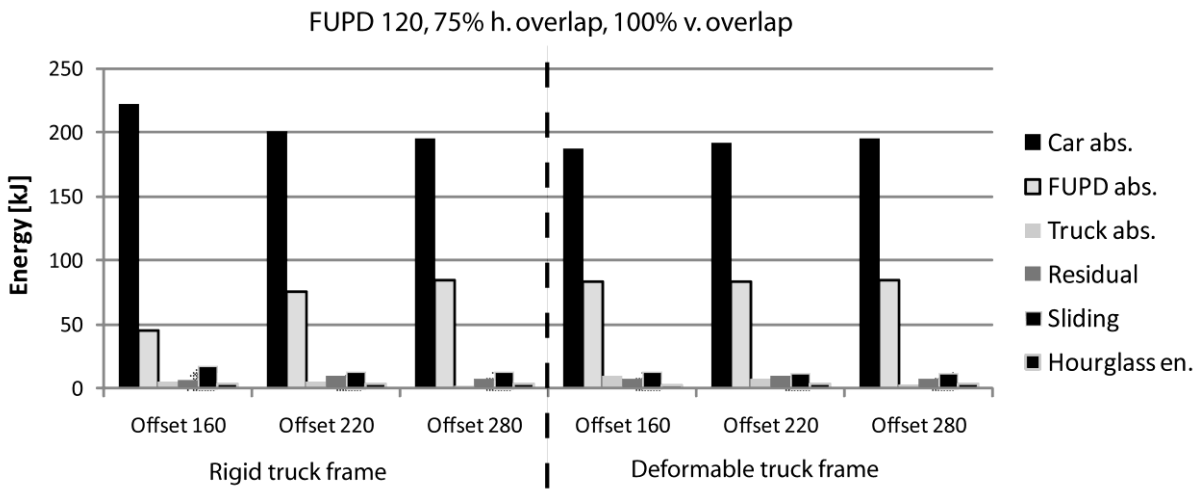

Figure 17

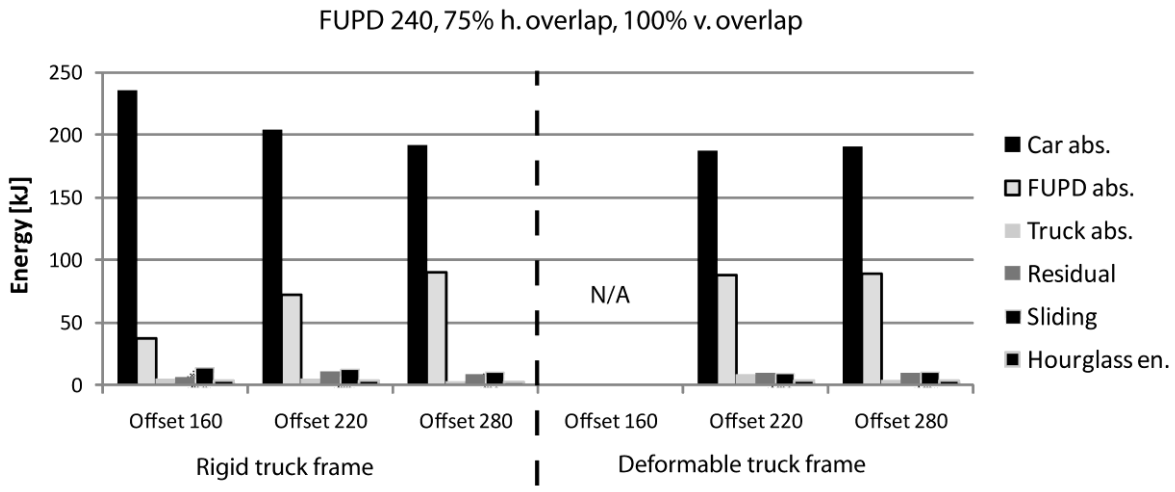

Figure 18

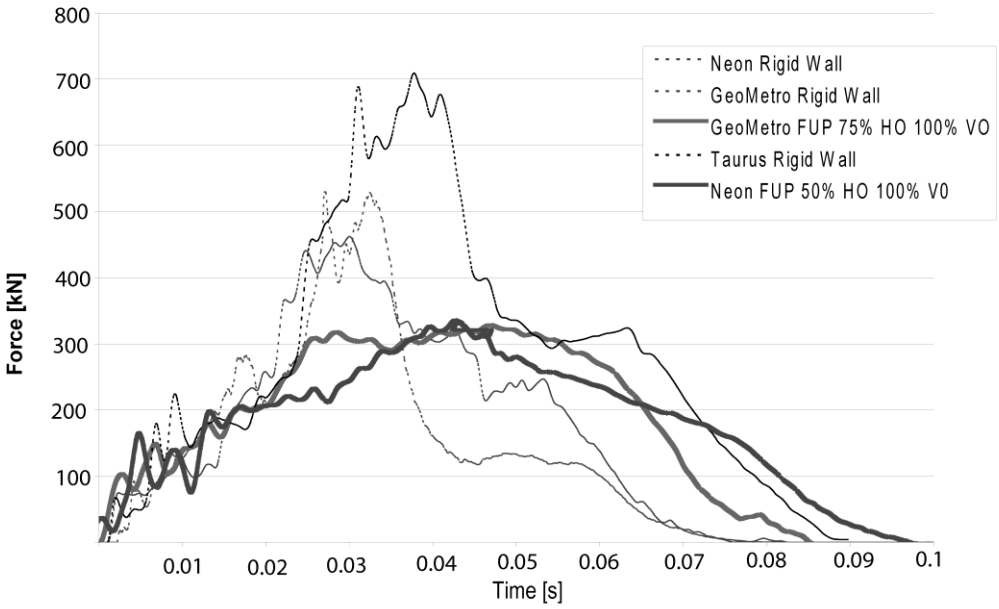
800
700
600
500
400
300
200
100
Force [kN]
0.01
0.02
0.03
0.04
0.05
0.06
0.07
0.08
0.09
0.1
Time [s]
Neon Rigid Wall
GeoMetro Rigid Wall
GeoMetro FUP 75% HO 100% VO
Taurus Rigid Wall
Neon FUP 50% HO 100% V0

Figure 19